CALCULATION METHOD OF MILLING CONTACT AREA FOR BALL-END MILLING TOOL WITH TOOL INCLINATION ANGLE

Yishu HAO[1], Guoqing TANG[2], Meng ZHANG[3]

Milling contact area of ball-end milling tool is studied when tool axis is not parallel to machining surface normal. Based on micro milling force modeling, cutting edge is divided into cutting edge elements along the axis direction by differential. The boundary equation is derived through analytical method. Line integral along cutting edge is used to obtain the whole milling contact area. According to the proposed calculation program of integration interval with tool inclination angle, virtual slot cutting experiment is done. Compared with published experimental results, the accuracy of proposed integration interval searching algorithm and milling force calculation program are verified.

Keywords: contact area; ball-end milling tool; tool inclination angle

1. Introduction

With the rapid development of aerospace, precision parts and health care, aluminum alloy with high strength, high toughness, anti-corrosion is becoming a key material. To machine-tool system, the main sources of error in machining process are the geometry and kinematics error of CNC machine, the thermal deformation of process system and the force deformation of process system. Geometry and control system error of machine tool accounts for 18% of the final machining error, error caused by heat accounts for 6%, and surface position error caused by milling force accounts for 76%, so the error caused by milling force is the main source of error[1].

The prediction of cutting forces in five-axis ball-end milling of free-form surfaces requires not only comprehensive modeling of cutting mechanics in three directions, but also the modeling of feed variation contributed by three linear and two rotary motions of the machine tool[2]. For ball-end milling tools, the cutting speed of each element edge is constantly changing [3], and shear force of differential edge is directly related to the milling speed[4]. In slot cutting experiment, the tool spindle perpendicular to the surface of workpiece. Milling

[1] Prof., School of Mechanical Engineering, Tongji University, China, e-mail: yishu@tongji.edu.cn
[2] Master, Tongji University, China, e-mail: tangguoqing1001@gmail.com
[3] Master, Tongji University, China, e-mail: zhangmengtongji@sina.com

tool from the tip position to the maximum depth of cut is involved in cutting, through changing the axial cut depth of cutting tool, the relationship between the position of the cutting unit on the cutting edge and the milling force coefficient can be determined. Some scholars take axial depth as polynomial independent variable[5], some take cutting thickness and axial depth as variables to fit milling force coefficient[6], thus to calculate milling force, all of them has acquired high calculation accuracy.

Due to variable tool axis orientation, free form surfaces of workpiece and tool geometry, engagement regions between the tool and the workpiece all along the tool path are very complex and irregular [7]. At present, the main calculation methods of tool-workpiece contact area are Z-map method and analytical method. Z-map method[8] expresses machined surface through using different height values on the corresponding X-Y grid, then tool-workpiece contact area is obtained by intersecting swept volume which is generated on the basis of tool path and tool geometry. Although Z-map method can be effectively applied in machining process modeling for complex curved surface, it occupies more computing time when calculating contact area [9]. Analytical method calculates the tool-workpiece contact area through solving workpiece surface equation and tool geometrical equation.

Based on micro milling force modeling theory, cutting edge of ball-end milling tool is divided into cutting edge element along the axis direction by differential in this paper. The boundary equation of contact area when tool axis is not parallel to the surface normal is deduced through analytical calculation.

2. Calculation of milling contact area for ball-end milling tool

2.1 Model of milling process for ball-end milling tool

Milling force on the edge line involved in cutting can be obtained by integrating micro milling force on the edge line along the cutting edge. The integration interval is the contact area of milling tool and workpiece.

Line integral method along the cutting edge, which is a spiral line shown in fig.1, is used in this paper to calculate the entire milling force. Only one integral limit is required to calculate at every corner position, so it has high computational efficiency.

Suppose the curvature radius of the machined surface is far greater than the spherical radius of ball-end milling tool, that is the workpiece's surface is a plane. Take tool angle θ as abscissa, the distance along the tool axis away from tool tip Z as ordinate, set up coordinate system (θ, Z) as shown in fig.2.

When the tool axis is not parallel to the surface normal, the machining surface equation is the region between the contact start corner θ_{st} and the end corner θ_{gx} of the line parallel to the abscissa line. The boundary of

tool-workpiece contact surface in (θ, Z) coordinate system is the rectangular area ABCD shown in fig.2. Spiral line equation shown in fig.1 is a slash in (θ, Z) coordinate system. The edge line of ball-end milling tool intersects contact boundary at two points, Z coordinate values of these two points are the upper and lower limit of integral.

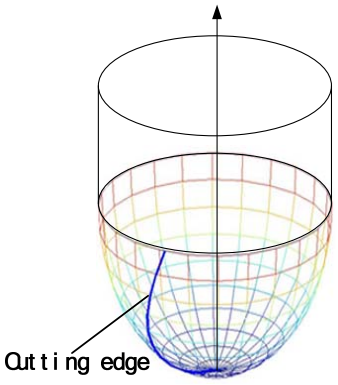

Fig.1. Spiral edge line

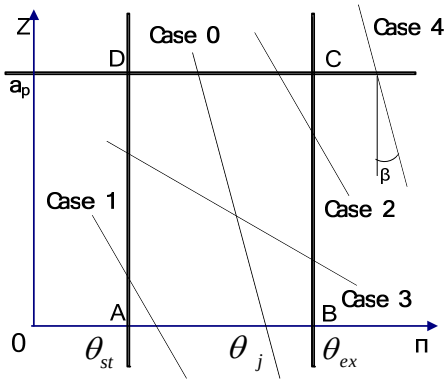

Fig.2. Coordinate system and integral interval

For the case when tool axis is parallel to the surface normal, the upper and lower limit of integration interval can be judged according to different positions between the edge line and contact area boundary. As shown in fig.2, the integral limits of different conditions are calculated as follows.

If $\theta_{st} < \theta_j(z = 0) < \theta_{gx}$,

$$Z_{j,1} = 0 \tag{1}$$

Case 0, if $\theta_{st} < \theta_j(z = 0) < \theta_{gx}$,

$$Z_{j,2} = a_p \tag{2}$$

Case 1, if $\theta_j(z = a) < \theta_{st}$,

$$Z_{j,2} = (1/k_\beta)(\theta + j\theta_p - \theta_{st}) \tag{3}$$

if $\theta_j(z = 0) > \theta_{gx}$ and $\theta_j(z = a) < \theta_{gx}$,

$$Z_{j,1} = (1/k_\beta)(\theta + j\theta_p - \theta_{gx}) \tag{4}$$

Case 2, if $\theta_j(z = a) > \theta_{st}$,

$$Z_{j,2} = a_p \tag{5}$$

Case 3, if $\theta_j(z = a) < \theta_{st}$,

$$Z_{j,2} = (1/k_\beta)(\theta + j\theta_p - \theta_{st}) \quad (6)$$

Case 4, if $\theta_j(z=0) < \theta_{gx}$ and $\theta_j(z=a) > \theta_{gx}$, the spiral groove will be divorced from the cutting zone.

Here θ_{st} is the contact start corner, θ_{gx} is the contact end corner, θ_j of the point which is on the jth edge line meets

$$\theta_j = \theta_j(z) \quad (7)$$

β is tool's spiral angle, the slope of the spiral angle meets

$$k_\beta = \frac{\tan\beta}{R_0} \quad (8)$$

When tool axis is not parallel to the surface normal as is shown in fig.3. The machined surface is no longer a straight line parallel to the abscissa.

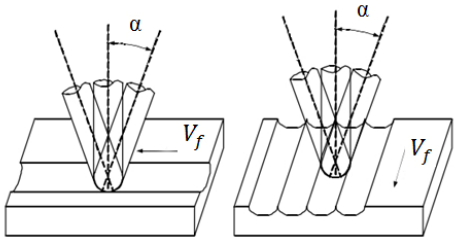

Fig.3. Tool axis and surface normal is not parallel

2.2 Calculation method of milling contact area with tool inclination

Through geometrical derivation, boundary height value of the contact area is expressed as a equation of tool corner θ.

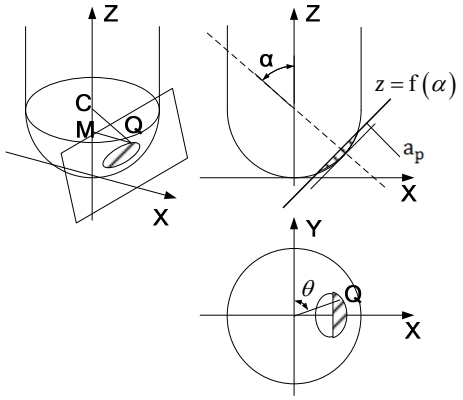

Fig.4. Contact area of tool and workpiece with inclination

In X-Y-Z system established on the basis of ball-end milling tool micro milling force model, the feed direction of ball-end milling tool is the positive

direction of X-axis. When ball-end milling tool turns an α angle around the line which inclines to the surface to be processed and parallel to Y-axis, and the workpiece surface intersects the spherical surface to produce a round. Then the spherical surface is divided into two parts, the small part is contact area of tool and workpiece as the shadow part shown in fig.4.

Suppose α is positive when ball-end milling tool inclines to the feed direction. The actual contact area is the half of contact surface at the milling direction side. The projection of workpiece surface on X-Z plane is a straight line. Suppose the cutting depth is a_p, then the equation of the projection line:

$$z = \mathrm{f}(\alpha) = \tan\alpha x + R_0 - \frac{R_0 - a_p}{\cos\alpha} \tag{9}$$

Suppose Q is a point on the upper side of the contact area boundary, namely the point is on the intersection's circular boundary of workpiece surface and spherical surface, the X coordinate of the point:

$$x = \frac{z - R_0 + \dfrac{R_0 - a_p}{\cos\alpha}}{\tan\alpha} \tag{10}$$

Connect spherical surface center point C and Q, make a vertical through Q to the tool axis, the vertical intersect Z-axis at point M, and a right-angled triangle CMQ can be gotten, where

$$CP^2 = MP^2 + CM^2 \tag{11}$$

According to fig.4, $\mathrm{CM} = \mathrm{R_0} - \mathrm{z}$, $\mathrm{CQ} = \mathrm{R_0}$,

$$\mathrm{MQ} = \sqrt{R_0^{\,2} - (R_0 - z)^2} \tag{12}$$

and for Q,

$$|x| = |MQ\sin\theta| \tag{13}$$

Substitute equation (10) and (12) into equation (13), and

$$|\sqrt{R_0^{\,2} - (R_0 - z)^2}\sin\theta| = |\frac{z - R_0 + \dfrac{R_0 - a_p}{\cos\alpha}}{\tan\alpha}| \tag{14}$$

Solve the quadratic equation of one unknown and round solutions that do not meet the practical significance,

$$z = R_0 + \frac{-\dfrac{R_0 - a_p}{\cos\alpha} + \sqrt{R_0^{\,2}\tan^2\alpha\sin^2\theta - \tan^2\alpha\sin^2\theta(\dfrac{R_0 - a_p}{\cos\alpha})^2 + R_0^{\,2}\tan^4\alpha\sin^4\theta}}{1 + \tan^2\alpha\sin^2\theta} \tag{15}$$

Similarly, the lower side boundary equation on the X-Z plane meets

$$z = -\cot\alpha x + R_0 \tag{16}$$

So for one point on the line,

$$x = \frac{R_0 - z}{\cot\alpha} \tag{17}$$

Connect this point and the spherical surface center C, make a vertical through it to the tool axis, intersects the tool axis at M,

$$|\sqrt{R_0^2 - (R_0 - z)^2}\sin\theta| = |\frac{R_0 - z}{\cot\alpha}| \tag{18}$$

Solve the quadratic equation of one unknown and round solutions that do not meet the practical significance,

$$z = R_0 - \frac{R_0\cot\alpha\sin\theta}{\sqrt{1+\cot^2\alpha\sin^2\theta}} \tag{19}$$

Different inclination directions correspond to different tool and workpiece contact situations. When $a_p \le R_0 - R_0\cos\alpha$, if the feed direction and the inclination direction are in the same plane, as is shown in fig.5. When $\alpha > 0$

$$\theta_{st} = \frac{\pi}{2} - \arctan\frac{\sqrt{R_0^2 - (R_0 - a_p)^2}}{(R_0 - a_p)\sin\alpha},\quad \theta_{ex} = \frac{\pi}{2} + \arctan\frac{\sqrt{R_0^2 - (R_0 - a_p)^2}}{(R_0 - a_p)\sin\alpha} \tag{20}$$

When $\alpha < 0$,

$$\theta_{st} = \frac{3\pi}{2} - \arctan\frac{\sqrt{R_0^2 - (R_0 - a_p)^2}}{(R_0 - a_p)\sin\alpha},\quad \theta_{ex} = \frac{3\pi}{2} + \arctan\frac{\sqrt{R_0^2 - (R_0 - a_p)^2}}{(R_0 - a_p)\sin\alpha} \tag{21}$$

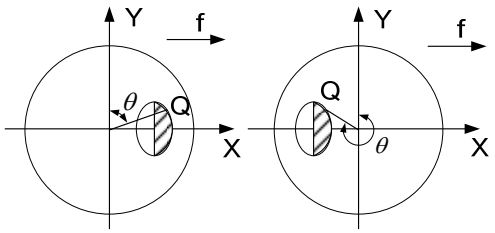

(a) $\alpha > 0$ (b) $\alpha < 0$

Fig.5. When $a_p \le R_0 - R_0\cos\alpha$, feed and inclination direction in the same plane

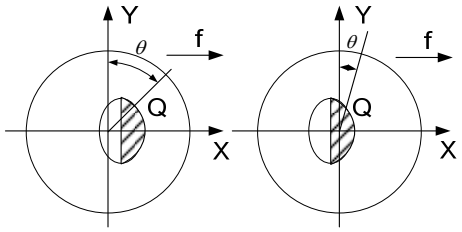

(a) $\alpha > 0$ (b) $\alpha < 0$

Fig.6. When $a_p > R_0 - R_0\cos\alpha$, feed and inclination direction in the same plane

When $a_p > R_0 - R_0\cos\alpha$, if the feed direction and the inclination direction are in the same plane, as is shown in fig.6.

When $\alpha > 0$

$$\theta_{st} = \frac{\pi}{2} - \arctan\frac{\sqrt{R_0^2 - (R_0 - a_p)^2}}{(R_0 - a_p)\sin\alpha},\quad \theta_{ex} = \frac{\pi}{2} + \arctan\frac{\sqrt{R_0^2 - (R_0 - a_p)^2}}{(R_0 - a_p)\sin\alpha} \tag{22}$$

When $\alpha < 0$

$$\theta_{st} = 0, \quad \theta_{ex} = 2\pi \tag{23}$$

When $a_p < R_0 - R_0 \cos\alpha$, if the feed direction is vertical to the inclination direction, as is shown in fig.7. when $\alpha > 0$

$$\theta_{st} = 0, \quad \theta_{ex} = \arctan \frac{\sqrt{R_0^2 - (R_0 - a_p)^2}}{(R_0 - a_p)\sin\alpha} \tag{24}$$

When $\alpha < 0$

$$\theta_{st} = \pi - \arctan \frac{\sqrt{R_0^2 - (R_0 - a_p)^2}}{(R_0 - a_p)\sin\alpha}, \quad \theta_{ex} = \pi \tag{25}$$

When $a_p > R_0 - R_0 \cos\alpha$, if the feed direction is vertical to the inclination direction, as is shown in fig.8,

$$\theta_{st} = 0, \quad \theta_{ex} = \frac{\pi}{2} \tag{26}$$

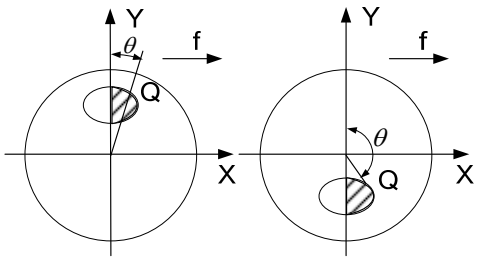

(a) $\alpha > 0$ (b) $\alpha < 0$

Fig.7. When $a_p < R_0 - R_0 \cos\alpha$, feed direction is vertical to inclination direction

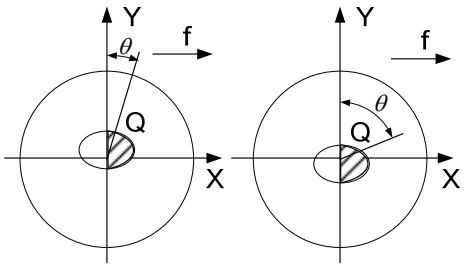

(a) $\alpha > 0$ (b) $\alpha < 0$

Fig.8. When $a_p > R_0 - R_0 \cos\alpha$, feed direction is vertical to inclination direction

Take the situation of $a_p \le R_0 - R_0 \cos\alpha$ as an example, the feed direction and the inclination direction are in the same plane, and the feed direction corresponds to the inclination direction. The actual position of tool-workpiece contact area is shown in fig.9. Z_1 is the lower boundary of contact area, Z_2 is the upper boundary of the contact area, the actual contact area is sandwiched between θ_{st} and θ_{ex} of the upper and lower contact boundary region.

When the tool axis of ball-end milling tool is parallel to the surface normal of the workpiece, the integral interval can be judged and calculated by simple conditions. When the tool axis is not parallel to the surface normal, suppose the edge line equation intersects the boundary of contact area at (θ_{i1}, z_1) and (θ_{i2}, z_2), $[z_1, z_2]$ is the required integral interval. Because the boundary equation of edge projection and contract area cannot be calculated directly, a search algorithm method is designed to search the intersections of edge line equation and

contact area boundary along the projection curve.

Set θ as tool corner, boundary of tool-workpiece contact area is shown in fig.10, in (θ, Z) coordinate system, $z = Z_1(\theta)$ is the lower side boundary equation, $z = Z_2(\theta)$ is the upper side boundary equation, $z = Z_3(\theta)$ is the edge line equation, $z = Z_1(\theta)$ intersects $z = Z_3(\theta)$ at (θ_{i1}, z_1), $z = Z_2(\theta)$ intersects $z = Z_3(\theta)$ at (θ_{i2}, z_2), z_{st} is the Z coordinate of the contact area start.

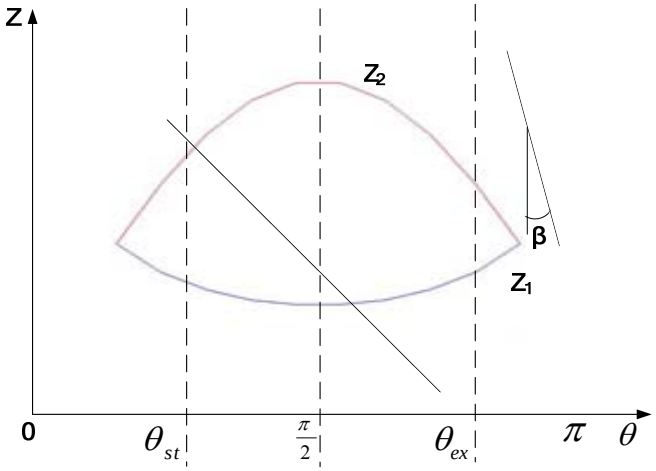

Fig.9. Integration interval when $a_p \le R_0 - R_0\cos\alpha$ and the feed direction is consistent with the inclination direction

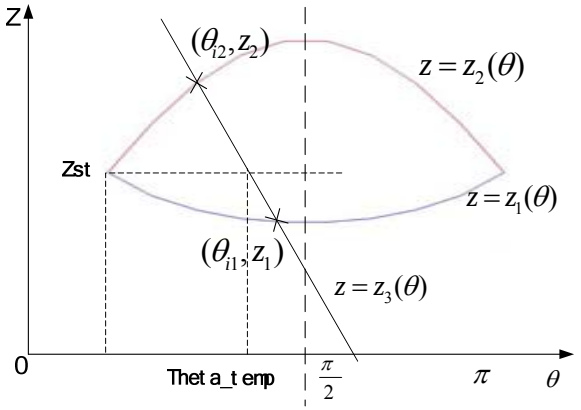

Fig.10. Search algorithm diagram when $a_p \le R_0 - R_0\cos\alpha$ and the feed direction is consistent with the inclination direction

The algorithm flow chart of range-searching (θ_{i1}, z_1) is shown in fig.11, here ignores the effect of contact start corner and contact end corner to the

position of (θ_{i1}, z_1), where k is the slope of edge line equation.

In the algorithm, judging the value Z_1 and Z_2 with the error limit of 10^{-2} mm will exist a certain error. Z_1 and Z_2 are the intersections of edge line and contact area boundary.

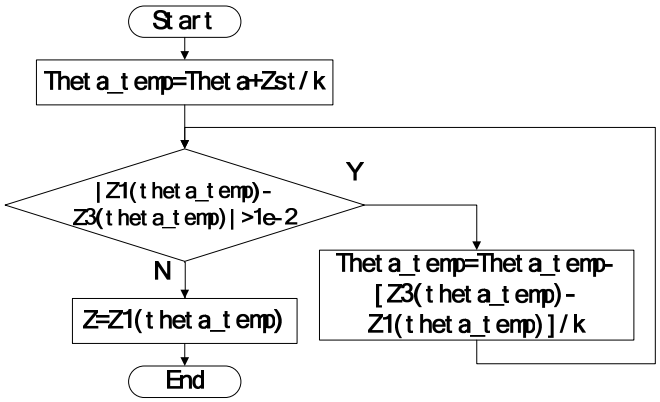

Fig.11. Searching algorithm flow chart when $a_p \le R_0 - R_0 \cos\alpha$ and the feed direction is consistent with the inclination direction

3. Verification of milling force results for ball-end milling tool

Altintas and Lee[10] used integral method to calculate the micro milling force of ball-end milling tool, and did experimental verification for ball-end milling force model they proposed on a single-edged ball-end milling tool. The workpiece material was titanium alloy (Ti6Al4V), the cutting force coefficient of the workpiece and cutting tool obtained in the experiment was explained.

Calculation program considering integral limit of inclination is used in this paper, and virtual groove cut simulation experiment is done according to the same cutting parameters and machining conditions, compared with the published experimental results, the calculation accuracy of the proposed integral interval searching algorithm and milling force calculation program can be verified.

The smooth lines are the milling force results use the calculation algorithm proposed in this paper. The corrugated lines are the experimental results in Altintas and Lee's paper.

Fig.12 shows the milling force of R_0=9.5 mm ball-end milling tool when spindle speed n=269 rpmin, feed rate per tooth f_z=0.05 mmptooth, axial cutting depth a_p=1.27 mm and 6.35 mm.

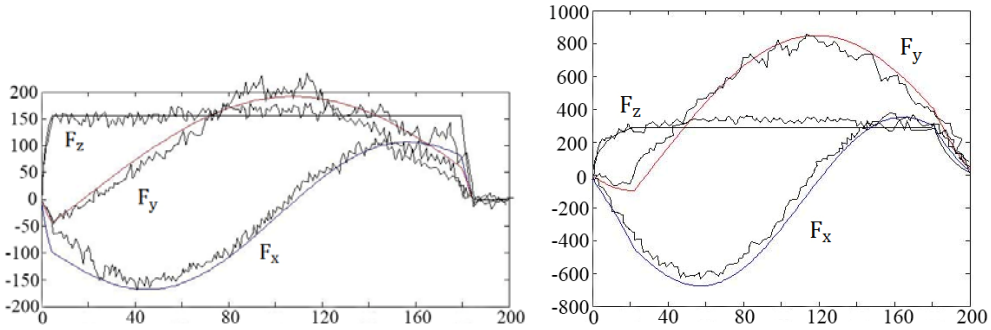

(a) a_p =1.27 mm (b) a_p =6.35 mm

Fig.12. When $\alpha_n = 0°$, Spindle speed n=269 rpmin, R_0=9.5 mm, β_0=30°, f_z=0.05 mmptooth

Fig.13(a) shows the milling force of R_0=9.5 mm ball-end milling tool when spindle speed n=269 rpmin, axial cutting depth a_p =3.81 mm, feed rate per tooth f_z=0.10 mmptooth. Fig.13(b) shows the milling force of R_0=6.5 mm ball-end milling tool when spindle speed n=269 rpmin, axial cutting depth a_p =3.04 mm, feed rate per tooth f_z=0.08 mmptooth.

Fig. 13(a) shows the maximum Y direction milling force in the experiment is about 900 N, the maximum Z direction milling force is about 400 N, and in this paper the maximum error of calculated milling force in Y direction is about 12.5%, maximum error of milling force in Z direction is about 30%.

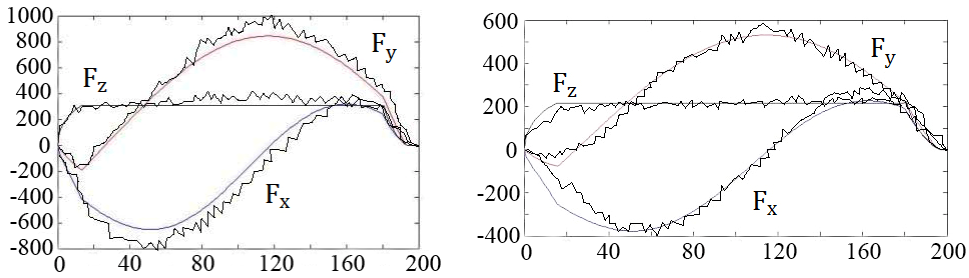

(a) a_p =3.81 mm, R_0=9.5 mm, f_z=0.10 mmptooth

(b) a_p =3.048 mm, R_0=6.5 mm, f_z=0.08 mmptooth

Fig.13. Spindle speed n=269 rpmin, β_0=30°

Fig.14 shows results of machining experiment when contact angle is 0-90°, and the milling force of ball-end milling tool when the spindle speed n=269 rpmin, R_0=9.5 mm, axial cutting depth a_p =6.35 mm, feed rate per tooth f_z=0.05 mmptooth and f_z=0.10 mmptooth.

The calculated milling force in this paper has obvious errors after 60°

corner in Y and Z direction, and milling force in Y and Z direction appear sharp angle at 90°.

The possible sharp angle position by numerical calculation in slot cutting is the corner of 180°, in semi-slot cutting is 90°, they are all in the position of milling edges begin to leave the milling areas. Using the error limit of 10^{-2} mm as a judgment in the program, when improve judgment accuracy, sharp angle can be significantly reduced.

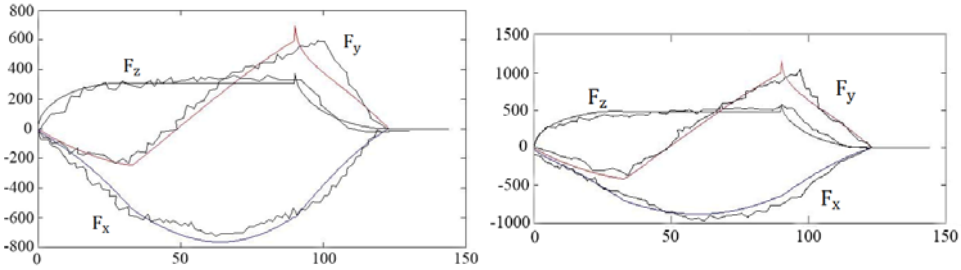

(a) f_z=0.05 mmptooth (b) f_z=0.10 mmptooth

Fig.14. Semi-slot cutting, spindle speed n=269 rpmin, a_p=6.35 mm, β_0=30°

Using the proposed milling force calculation program, which takes tool inclination into consideration, to calculate the milling force corresponding to different milling parameters when α =0°. The error is relatively large during cutting-in and cutting-out process. When the maximum milling force is very large, the error of the milling force is obvious.

4. Conclusions

The calculation of milling force is based on micro milling force modeling theory. Integrating the milling force of micro cutting edges along the contact edge line between tool and workpiece, milling force in specific contact conditions can be gotten. Geometric analytical method is used to calculate boundary equations of contact area when tool axis of ball-end milling tool is not parallel to the machining surface normal. The calculation results of milling force through numerical optimization are compared with foreign research results proposed calculation method has higher accuracy in finishing process.

REFERENCES

[1]. *Tony L.Schmitz, John C. Ziegert, J.Suzanne Canning, Raul Zapata.* "Case study: A comparison of errors sources in high-speed milling", Precision Engineering, vol.32, pp.126-133, 2008.

[2]. *Oguzhan Tuysuz,Yusuf Altintas, Hsi-Yung Feng*. "Prediction of cutting forces in three and

five-axis ball-end milling with tool indentation effect", International Journal of Machine Tools and Manufacture, vol.66, pp.66-81, 2013.

[3]. *E.J.A.Armarego, R.C.Whitfield.* "Computer based modeling of popular machining operations for forces and power prediction", Annals of the CIRP, vol.34, No.1, pp.65-69, 1985.

[4]. *T.Hosoi.* "Cutting action of ball end mill with a spiral edge", Annals of the CIRP, vol.25, No.1, pp.49-53, 1997.

[5]. *Abrari F, Elbestawi M A, Spence A D.* "On the dynamics of ball End Milling: Modeling of Cutting Forces and Stability Analysis", International Journal of Machine Tools and Manufacture, vol.38, pp.215-237, 1998.

[6]. *Jung Y H, Kim J S, Hwang S M.* "Chip load prediction in ball-end milling", Journal of Materials Processing Technology, vol.111, pp. 250-255, 2001.

[7]. *I. Lazoglu, Y. Boz, H. Erdim*. "Five-axis milling mechanics for complex free form surface", CIRP Annals-Manufacturing Technology, vol.60, pp.117-120, 2011.

[8]. *Fussell B K, Jerard R B, Hemmett J G..* "Modeling of cutting geometry and forces for 5-axis sculptured surface machining", Computer Aided Design, vol.35, No.4, pp.333-346, 2003.

[9]. *Zhang Chen, Zhou Rurong, Zhuang Haijun, Zhou Laishui.* "Modeling and Simulation of Ball end Milling Forces Based on Z-map Model", Acta Aeronautica Et Astronautica Sinica, vol.27, No.2, pp. 347-352, 2006.

[10]. *Y.Altintas, P.Lee.* "Mechanics and Dynamics of Ball End Milling", ASME Journal of Manufacturing Science and Engineering, vol.120, pp. 684-692, 1998.